Journal of Biomedical Science (2007) 14:681–694
DOI 10.1007/s11373-007-9165-3

Apoptotic cleavage of NuMA at the C-terminal end is related to nuclear disruption and death amplification

Hsueh-Hsuan Lin[1], Hsin-Ling Hsu[1,2] & Ning-Hsing Yeh[1,*]
[1]*Institute of Microbiology and Immunology, School of Life Science, National Yang-Ming University, 155 Li-Nong Street Sec. 2, Taipei, 112, Taiwan ROC;* [2]*Division of Molecular and Genomic Medicine, National Health Research Institutes, 35 Keyan Road, Zhunan Town, Miaoli County, 350, Taiwan ROC*

Received 31 October 2006; accepted 5 March 2007

Key words: apoptosis, caspase, chromatin condensation, micronucleation, nuclear matrix, nucleus, NuMA

Abstract

NuMA is a nuclear matrix protein in interphase and distributes to the spindle poles during mitosis. While the essential function of NuMA for mitotic spindle assembly is well established, a structural role of NuMA in interphase nucleus has also been proposed. Several observations suggest that the apoptotic degradation of NuMA may relate to chromatin condensation and micronucleation. Here we demonstrate that four apoptotic cleavage sites are clustered at a junction between the globular tail and the central coiled-coil domains of NuMA. Cleavage of a caspase-6-sensitive site at D^{1705} produced the R-form, a major tail-less product of NuMA during apoptosis. The other two cleavage sites were defined at D^{1726} and D^{1747} that were catalyzed, respectively, by caspase-3 and an unknown aspartase. A NuMA deletion mutant missing the entire cleavage region of residues 1701–1828 resisted degradation and protected cells from nuclear disruption upon apoptotic attack. Under such conditions, cytochrome *c* was released from mitochondria, but the subsequent apoptotic events such as caspase-3 activation, poly(ADP-ribose) polymerase degradation, and DNA fragmentation were attenuated. Conversely, the tail-less NuMA alone, a mutant mimicking the R-form, induced chromatin condensation and activated the death machinery. It supports that intact NuMA is a structural element in maintaining nuclear integrity.

Introduction

Nuclear-mitotic apparatus protein (NuMA) is a component of the nuclear matrix with cell cycle-dependent distribution patterns. In interphase, NuMA is present in the non-nucleolar regions of nuclei. During mitosis, it is translocated to the centrosomal regions of the mitotic apparatus. The NuMA molecule consists of the globular head and tail domains, and the central discontinuous α-helical coiled coils [1], a structural organization similar to that of the intermediate filament family proteins [2, 3]. Most known functional motifs or regions of NuMA are localized in the C-terminal globular tail, including a nuclear localization signal motif (NLS) [4, 5], four Cdc 2 phosphorylation sites [6], a spindle-association domain [5, 7], and binding domains for interaction with a diverse type of cellular proteins [8–10].

Functions of NuMA for spindle assembly during mitosis have been well established [11–13]. However, several observations suggested that NuMA could also regulate the nuclear structural integrity in interphase. For examples, micronucleated cells were induced by microinjection of NuMA antibodies [14], or by expression of different tail-truncated NuMA proteins [4].

*To whom correspondence should be addressed. Fax: +886-2-28212880; E-mail: yphcsl@ym.edu.tw

The appearance of a tail-less NuMA, namely R-form, was correlated with the oligonucleosomal laddering and nuclear fragmentation during apoptosis [15]. We hypothesize that NuMA cleavage is a common consequence of apoptosis that contributes to nuclear disruption. It has been demonstrated that NuMA is cleaved by granzyme B and caspase-3 to generate distinct cleavage fragments [16], and that the cleavage products of NuMA catalyzed by caspase-3 or caspase-6 were different in sizes [17]. Furthermore, different protease inhibitors such as *N*-tosylphenylalanine chloromethylketone, iodoacetamide, and synthetic tetrapeptide blockers specific to caspase-3 or caspase-6 suppressed the cleavage of NuMA upon apoptotic induction [16–18]. Additionally, NuMA was not cleaved in caspase-3 null MCF7 breast cancer cells [19], but the cleavage was restored in the stable clones of MCF7 expressing procaspase-3 during staurosporine-induced apoptosis [20]. These observations imply that there are caspase-dependent and independent pathways for NuMA cleavage at multiple positions. One apoptotic cleavage site upon drug treatment has been mapped to the globular tail of NuMA ranging from residues 1701 to 1725 [18]. Furthermore, overexpression of the full-length NuMA led to the formation of a quasi-hexagonal lattice-like structure in the nucleus [21]; bacterially expressed NuMA underwent self-assembly into multiarm oligomers *in vitro* [22]. On the other hand, silencing of NuMA gene by RNA interference resulted in apoptotic phenotypes [23]. These findings suggest that NuMA with its unique molecular features may play a structural role in cell nucleus.

Here, we demonstrate that there are four apoptotic cleavage sites in the globular tail region of NuMA within amino acid residues 1701–1828. Cleavage at D^{1705} generates the R-form of NuMA during apoptosis. Upon apoptotic attack, an uncleavable mutant of NuMA does not prevent the early apoptotic event of cytochrome *c* release, but protects cells from nuclear disruption and blocks subsequently the apoptotic amplification. Cells overexpressing a tail-less NuMA, a mutant mimicking the R-form of NuMA, exhibit chromatin condensation and gain apoptotic phenotypes. These findings imply that intact NuMA plays an important role in organizing the nuclear structure in interphase.

Materials and methods

Cell cultures, antibodies, and reagents

HeLa Tet-Off cell line (tHeLa, a cervical epitheloid carcinoma cell line carrying the tetracycline repressor gene *TetR*; Clontech) and 293T cells (an embryonic kidney cell line carrying the SV40 large T antigen) were grown in RPMI 1640 medium (GIBCO-BRL) and Dulbecco's Modified Eagle medium (GIBCO-BRL), respectively; both media were supplemented with 10% fetal bovine serum (GIBCO-BRL). Monoclonal antibodies (mAb) used included HS87 (IgG1, anti-NuMA) [15], LL1 (IgG1, anti-Ku80 for immunoblotting) [24], BL9 (IgG2a, anti-Ku80 for immunofluorescence staining) [24], CP2 (IgG2a, anti-hNopp140) [25], M2 (IgG1, anti-Flag; Sigma), and B-7 (IgG2a, anti-α-tubulin; Santa Cruz). The following polyclonal antibodies were also used: rabbit anti-poly(ADP-ribose) polymerase (PARP) p85 fragment (Promega), rabbit anti-active® caspase-3 (Promega), and sheep anti-cytochrome *c* (Calbiochem). Three apoptotic inducers, staurosporine (1 mM; Sigma), 5,6-dichloro-1-β-D-ribofuranosylbenzimidazole (DRB) (0.5 M; Sigma) and adriamycin (2 mg/ml; Sigma), a caspase-3 inhibitor benzyloxycarbonyl-Asp-Glu-Val-Asp-fluoromethylketone (z-DEVD-fmk) (40 mM; Stratagene) and a caspase-6 inhibitor benzyloxycarbonyl-Val-Glu-Ile-Asp-fluoromethylketone (z-VEID-fmk) (40 mM; Calbiochem) were dissolved in dimethyl sulfoxide as the stocks and stored in aliquots at −70 °C. All of the stock solutions were added directly to the tHeLa or 293T cell cultures at a final concentration as indicated in each experiment.

Drug treatments

Cells were grown to 30% confluence in 60 mm dishes or on microscopic coverslips placed in 35 mm dishes. On the next day, fresh medium was replenished 4 h before the beginning of each experiment. For apoptotic induction, cells were incubated in medium containing staurosporine (1 μM), DRB (0.25 mM), or adriamycin (4 μg/ml) for 12 h. For inhibitor studies, transfected tHeLa cells were pre-incubated with z-DEVD-fmk (100 μM) or z-VEID-fmk (100 μM) for 15 min. Then, staurosporine (1 μM) was added into

culture dishes in the presence of inhibitor for 12 h. For all experiments, cells in the dishes (both attached and floating) were harvested for preparation of cell lysates and cells on the coverslips (attached only) were subjected to immunofluorescence staining.

Mammalian expression constructs

Expression vector pFLAG-CMV2 (Sigma) or pFNLS (derived from pFLAG-CMV2) [26] were used to express Flag-tagged proteins. All constructs were generated with inserts located downstream and in frame with the Flag-epitope sequences. The full-length NuMA cDNA was made from a partial cDNA of NuMA, HS3 clone 1 (encoding amino acids 350–1738) [15]. The 5′-end complete cloning was accomplished by PCR amplification of a human leukemia, chronic myelogenous Marathon-Ready™ cDNA (Clontech), using a pair of primers (forward, 5′-CTGTCTGGCATCACCAAGATGACACTC-3′; reverse, 5′-TTCCTTGGCCTGGCTGAGGTTGGA-3′); this PCR-amplified 5′-fragment was ligated with the HS3 clone 1 to create the TM7 (encoding amino acids 1–1738). For cloning the missing 3′-end of NuMA, we generated cDNA fragment TM4 (encoding amino acids 1476–2115) by PCR amplification of a human HeLa 5′-STRETCH PLUS cDNA library (Clontech) with a primer set (forward, 5′-TATGTCCAAGAGTTGGCAGCCGTACGTG CT-3′; reverse, 5′-TTGGCTACTGTTGGCCTGGGAGCTGA-3′). The full-length NuMA cDNA was created by ligation of TM7 and TM4, and similarly, TM2 was derived from HS3 clone 1 and TM4. TM6 and TM5 were generated by PCR from the same HeLa cDNA library with the following paired primers: TM6 (forward, 5′-GACAGCGCCAACTCATCGTTCTAC-3′; reverse, 5′-TTGGCTATCGTTGGCCTGGGAGCTGA-3′) and TM5 (forward, 5′-TATGTC CAAGAGTTGGCAGCCGTACGTGCT-3′; reverse, 5′-TAGAGACTGAGTAGAGGAGGTGGCTCG-3′). TM3 was generated by PCR using HS3 clone 1 as the template with a primer set (forward, 5′-CGGGGTACCGCAACTTCAGGTGGCTAATGAA-3′; reverse, 5′-CTAGTCTAGAGGTGATACTGAGTGGGGTCCC-3′).

The full-length NuMA mutants (FL-D4A; FL-D1A; FL-D5A; FL-D4, 5, 8A; FL-D4, 5, 6, 8A; FL-D4, 5, 6, 7, 8A; FL-D5, 9A; FL-D4, 8A; and FL-D1, 4, 5, 8A), and the truncated NuMA mutants (TM4-D1A, TM4-D5A, TM4-D8A), were generated by QuickChange® Site-Directed Mutagenesis Kit (Stratagene) according to the manufacturer's protocol. The NuMA mutant TM1, missing amino acids 1701–1828, was generated by a strategy of overlapping PCR extension as described [27]. Briefly, the overlap-extension PCR used two external flanking primers (primer a: forward, 5′-TATGTCCAAGAGTTGGCAG CCGTACGTGCT-3′and primer d: reverse, 5′-TTGGCTACTGTTGGCCTGGGAGCTGA-3′) complementary to the NuMA sequences that are about 1.9-kb apart and flank the target deletion region, and two internal overlapping primers (primer b: reverse, 5′-***GAACGATGAGTTGGCGCTGTC***GAATTTGCCCAGGTCTCGAAGCTG-3′, and primer c: forward, 5′-***GACAGCGCCAACTCATCGTTC***TAC-3′; the bold-italic typefaces represent the overlapping primer sequences) that hybridize at sites across the deletion boundary. The two DNA products amplified from the TM4 template by using the two primer sets of (a + b) and (c + d) were fused after denaturing, annealing, and extension by *pfuTurbo*® DNA polymerase (Stratagene). Then, primers (a + d) were added into the mixture for PCR amplification (35 cycles). The PCR products (about 1.5-kb) were cloned into pGEM®-T Easy vector (Promega) and then constructed into a full-length variant, termed TM1, according to the standard cloning procedures. The TM4-D4A was also generated by methods of overlap-extension PCR [27], in which the mutant sequences were designed in the internal overlapping primers. As opposed to the other three site-directed mutagenesis products of TM4 (TM4-D1A, TM4-D5A, TM4-D8A), the ligation of the TM4-D4A into the pFlag-CMV2 vector created an additional loss of a 66-bp sequence at the multiple cloning sites. Therefore, the apparent molecular size of TM4-D4A is smaller than those of the other three TM4 mutants (see Figure 2C). All NuMA mutants generated by PCR were confirmed by DNA sequencing.

Transfection

Subconfluent cells (30% confluent) grown on glass coverslips were transiently transfected with purified plasmid DNA (2 μg per coverslip) by mixing with Lipofectamine (Invitrogen) according to the

manufacturer's protocol. The cells were analyzed by immunofluorescence staining 44 h after transfection. Calcium phosphate precipitation method was used for transfection of cells (30% confluent) grown on 60 mm dishes. Briefly, 6 μg plasmid DNA was dissolved in 50 μl of a 2 M $CaCl_2$ solution followed by the addition of TE buffer (10 mM Tris–HCl [pH 8.0], 1 mM EDTA) to a final volume 400 μl. This solution was added dropwise into 400 μl of HSD solution (50 mM HEPES, 0.28 mM NaCl, 1.5 mM Na_2HPO_4, 10 mM KCl, 12 mM dextrose). After 30 min of incubation at room temperature, the mixture was added dropwise to cells in a 60 mm dish containing 3 ml Dulbecco's Modified Eagle medium supplemented with 10% fetal bovine serum. After incubation at 37 °C for 20 h, cells were washed with phosphate-buffered saline (PBS). After adding 3 ml of fresh medium to each dish, the cells were returned to 37 °C incubation for another 24 h before preparation of cell lysates.

Immunoblot analysis

Cells were dissolved in Laemmli sample buffer and boiled for 10 min. Proteins were separated by SDS-PAGE and transferred to nitrocellulose filters. The filters were reacted with HS87 (anti-NuMA), LL1 (anti-Ku80), or M2 (anti-Flag) and then with peroxidase-conjugated goat anti-mouse IgG (Promega). The specific proteins were visualized by use of the enhanced chemiluminescence detection reagents (Amersham Biosciences).

Immunofluorescence staining and TUNEL assay

Cells grown on coverslips were fixed by 4% paraformaldehyde (Electron Microscopy Sciences) in PBS for 20 min at room temperature, followed by permeabilization with 0.2% Triton-X-100 for 5 min and washing once with PBS. Double immunofluorescence staining was performed as described [26]. For co-staining, the ectopically expressed Flag-tagged NuMA-derived proteins were detected by anti-Flag mAb M2 followed by fluorescein isothiocyanate (FITC)-conjugated goat anti-mouse IgG (Jackson), while the active caspase-3, the 85 kD fragment of PARP, or the endogenous cytochrome *c* were detected by specific polyclonal antibodies followed by a matched secondary antibody either rhodamine-conjugated goat anti-rabbit IgG (Jackson) or rhodamine-conjugated donkey anti-sheep IgG (Jackson). For double staining by mAb of subclasses IgG1 and IgG2a, the primary IgG1 antibody (anti-Flag) was detected by FITC-conjugated goat anti-mouse IgG1 (Caltag), whereas the primary IgG2a antibodies (specific to the hNopp140, Ku80, and α-tubulin) were probed with biotin-conjugated goat anti-mouse IgG2a (Caltag) followed by UltraAvidin™-rhodamine conjugate (Leinco). For co-staining of DNA, Hoechst 33258 (0.4 μg/ml; Sigma) was added to the last staining solution. Samples mounted in anti-fade solution [15] were analyzed under Olympus BX50 or BX51 epifluorescence microscopes, and were either photographed on Kodak Elite Chrome 400 films or converted to digital images through CoolSNAP *fx* CCD monochrome camera (Taiwan Instrument Co.).

The terminal deoxynucleotidyl transferase-mediated dUTP nick end labeling (TUNEL) assay was performed using Tdt-FragEL™ DNA Fragmentation Detection Kit (Oncogene) according to the manufacturer's instructions. The transfected cells, with or without treatment with apoptotic inducers during the last 12 h of incubation, were fixed and permeabilized as described above. Cells on the coverslips were subjected to TUNEL assay. Whether cells incorporated with biotin-conjugated dUTP were determined by UltraAvidin™-rhodamine conjugate (Leinco). Meanwhile, the Flag-tagged proteins were co-stained with M2 as described above.

Results

Mapping the apoptotic cleavage region of NuMA

We attempted to identify possible cleavage region(s) of NuMA during apoptosis by analyzing various truncated NuMA proteins. The tHeLa cells transiently transfected with constructs encoding the N-terminally Flag-tagged NuMA mutants, such as TM2 (head-less), TM3 (two-thirds of the central α-helical coiled coils), TM4 (globular tail together with a short C-terminal part of the coiled coils), TM5 (N-terminal half of the TM4), and TM6 (C-terminal half of the TM4) (Figure 1A), were incubated for 12 h with apoptotic inducers

either staurosporine, a protein kinase inhibitor, or adriamycin, a DNA damage agent (Figure 1B). The cleavage products generated from TM2, TM4, and TM5 were readily identified. In contrast, the cleaved TM3 was located only slightly lower than the uncleaved one, indicating that the cleavage site(s) should be near to the C-terminal end of TM3. However, TM6 remained intact under the same apoptotic conditions. Interestingly, the small fragments, TM4 and TM5, with a better resolution created four common cleavage products (30, 32, 34, and 41 kD; marked by open dots in lanes 10, 12, 16, and 18 of Figure 1B). Taken together, the immediately upstream region of the amino acid residue 1828 in NuMA molecule contains four cleavage sites. Previous studies have demonstrated that one apoptotic cutting site exists in the region of amino acids 1701–1725 of NuMA [18]. We therefore analyzed caspase recognition motifs present in the residues 1701–1828 of NuMA. According to the substrate specificities of the apoptotic caspases [28], this region was found to have one matched caspase-3 and two potential caspase-6 cleavage motifs (Figure 2A). In order to identify all possible cleavage sites, we also set forward to analyze the other six aspartates that match with no known consensus sequences for caspase cleavage.

Identification of the apoptotic cleavage sites on NuMA molecule

Site-directed mutagenesis was applied to replace aspartate with alanine in the potential cleavage region of NuMA. The nine aspartates in this region are numbered from 1 to 9 (Figure 2A). The full-length of NuMA (FL) with or without mutation at the aspartate residues were expressed by tHeLa cells and tested for the staurosporine-induced cleavage (Figure 2B). Results showed that the FL-D4A (single mutation at the caspase-3 cleavage site of D^{1726}), and FL-D4, 8A (double mutation at the caspase-3,-6 cleavage sites of D^{1726} and D^{1799}, respectively) produced the R-form of NuMA as did the wild-type FL after staurosporine treatment (Figure 2B, marked by solid dots in the lanes 2, 4, and 18). Thus, we excluded the D^{1726} and D^{1799} of NuMA as the cleavage site for generating the R-form, a major final cleavage product of NuMA during apoptosis [15]. On the other hand, after apoptotic cleavage, the FL-D1A (mutation at a predicated caspase-6 cleavage site of D^{1705}) lost the R-form but created new products with higher molecular sizes (Figure 2B, marked by the open dot in lane 6). These intermediate forms of NuMA were also accumulated upon apoptotic attack in cells overexpressing FL-D5A, FL-D4, 5, 8A (triple mutation), FL-D4, 5, 6, 8A (quadruple mutation), FL-D4, 5, 6, 7, 8A (quintuple mutation), and FL-D5, 9A (double mutation) (Figure 2B, lanes 8, 10, 12, 14, and 16; open dots). There was a tendency that, as long as the D^{1747} was replaced by alanine, the accumulation of the intermediate forms of NuMA was much obvious, likely due to attenuation of further degradation of the intermediate forms into the final R-form of NuMA. Importantly, the R-form of NuMA could still be derived from these five mutants but not from the FL-D1, 4, 5, 8A (quadruple mutation; Figure 2B, lane 20). We also found that the cleavage patterns of two NuMA double mutants, FL-D2, 5A and FL-D3, 4A, were identical, respectively, to those of the single mutants, FL-D5A and FL-D4A during the staurosporine-induced apoptosis (data not shown). It suggests that D^{1719} or D^{1723} are not sensitive to the apoptotic cleavage, and thereby, not the sites for production of the R-form. All above results support that D^{1705}, a potential caspase-6 cleavage site, is the target residue for generating the R-form of NuMA during apoptosis, and that there are more than one cleavage sites located downstream of D^{1705} for producing the intermediate forms during NuMA cleavage.

By calculation, the four apoptotic fragments derived from TM4 could be equivalent to sequences that start from Y^{1476} and extend downstream to the D^{1705} (30 kD), D^{1726} (32 kD), D^{1747} (34 kD), or D^{1799} (41 kD). To test these possibilities, the constructs encoding the truncated NuMA, TM4, with or without mutation at various aspartate residues were transfected into tHeLa cells for detecting their cleavage after induction by staurosporine for 12 h (Figure 2C). TM4 as the positive control was cleaved into 30, 32, 34, and 41 kD products during the staurosporine-induced apoptosis (Figure 2C, lane 2). Under the same condition, TM4-D1A (disruption of a caspase-6 cleavage site at D^{1705}) was only cleaved into 32, 34, and 41 kD products (Figure 2C, lane 4). Results of missing the 30 kD product, the smallest fragment, further support that D^{1705} is the cutting site as for generating the R-form of NuMA during

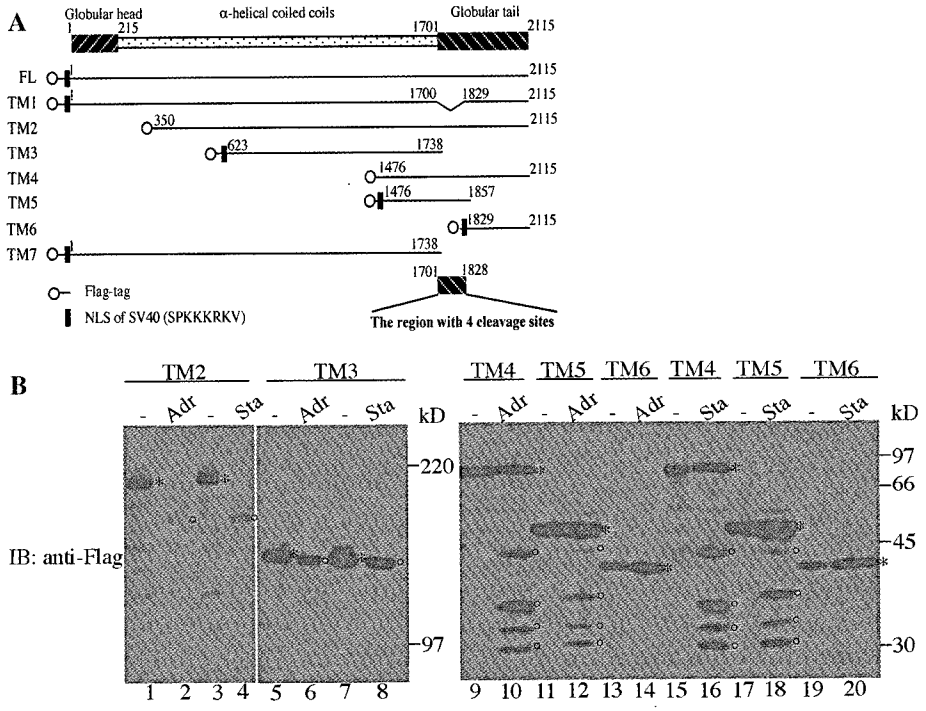

Figure 1. Apoptotic cleavage of truncated NuMA. (A) Schematic representation of the full-length NuMA and seven truncated NuMA proteins. The numbering system refers to the amino acid residues on NuMA. The Flag-tagged and the NLS of SV40 (SPKKKRKV) were constructed at the N-terminal ends in-frame to the coding regions. The apoptotic cleavage region (amino acids 1701–1828) of NuMA contains four cleavage sites (see the text). (B) Mapping the apoptotic cleavage region of NuMA. For the 44 h-transfection experiments, tHeLa cells overexpressing the truncated NuMA proteins, TM2, TM3, TM4, TM5, or TM6, were incubated in the absence (–) or presence of 4 μg/ml adriamycin (Adr), or 1 μM staurosporine (Sta), during the last 12 h. Floating and attached cells were harvested together for immunoblotting (5×10^5 cells/lane) using anti-Flag mAb. Asterisks mark the NuMA truncated mutants with expected molecular masses; open circles represent their apoptotic cleavage products.

apoptosis. In contrast, TM4-D4A (disruption of a caspase-3 cleavage site at D^{1726}) produced 30, 34, and 41 kD products during the staurosporine-induced apoptosis (Figure 2C, lane 6). Thus, D^{1726} is one of the intermediate cutting sites of NuMA during apoptosis. Likewise, TM4-D5A (modified at D^{1747}) generated 30, 32, and 41 kD cleavage products (Figure 2C, lane 8), indicating that D^{1747} is another intermediate cutting site of NuMA. However, TM4-D8A (modified at D^{1799}) was cleaved into 30, 32, 34, and 41 kD products during the staurosporine-induced apoptosis (Figure 2C, lane 10). Thus, D^{1799}, even being considered as a potential caspase-6 cutting site, was not involved in the apoptotic degradation. Nowadays the cutting site located downstream of D^{1747} for generating the 41 kD fragment is still unknown.

To further test whether these identified cutting sites of NuMA were sensitive to caspases, we analyzed effects of peptide inhibitors z-DEVD-fmk and z-VEID-fmk, specific to caspase-3 and caspase-6, respectively, on the staurosporine-induced cleavage of TM4-D1A and TM4-D4A. Elimination of the specific cleavage products by the inhibitors confirmed D^{1705} and D^{1726} as cleavage sites for caspase-6 and caspase-3, respectively (Figure 2D, lanes 8 and 5, respectively). Both inhibitors partially blocked the cleavage at D^{1747} (marked as "5"), but did not affect the appearance of the 41 kD fragment (marked as "x") (Figure 2D). Thus, these data indicate that D^{1747} is cleaved by an aspartase other than the caspase-3 and caspase-6, and that the fourth cutting site is not sensitive to caspase-3 or downstream activated caspases, likely caspase-independent.

A NuMA deletion mutant missing the amino acids 1701–1828 resists the cleavage and maintains the nuclear integrity upon apoptotic attack

We constructed a NuMA mutant missing the entire region of residues 1701–1828 (TM1) (see

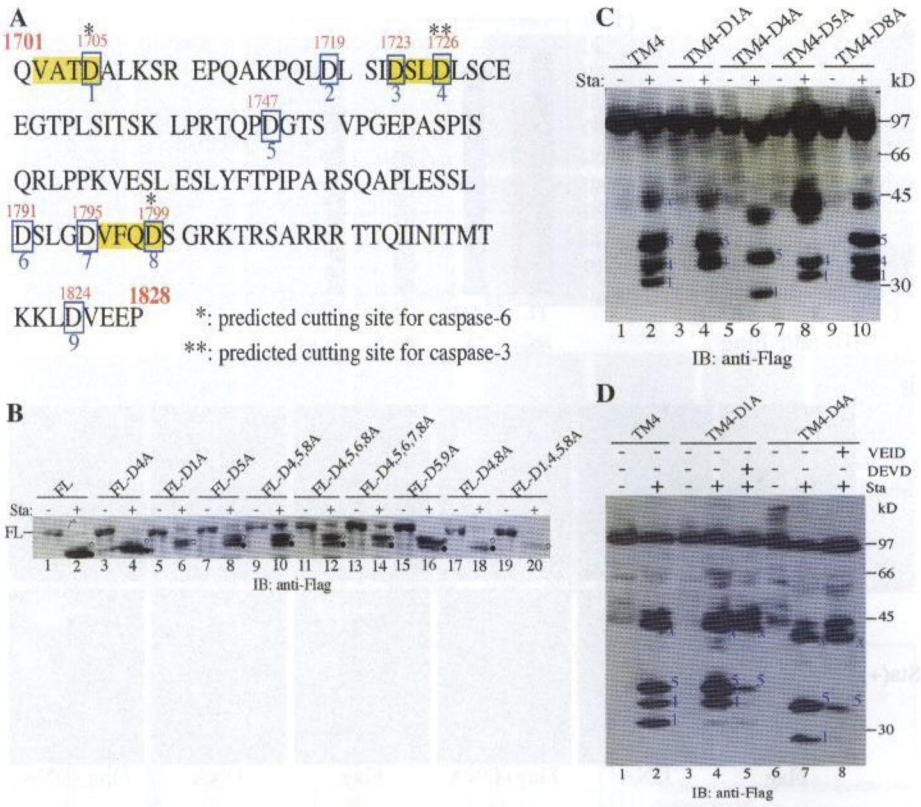

Figure 2. Mapping the apoptotic cleavage sites of NuMA. (A) The amino acid sequence of the apoptotic cleavage region of NuMA. This region (amino acids 1701–1828) contains one matched caspase-3 cutting site (**) and two potential caspase-6 cutting sites (*); the possible recognition motifs are highlighted in yellow. The nine aspartate residues in this region are boxed and numbered from 1 to 9. (B) The D^{1705} as the cutting site for generating the R-form of NuMA during apoptosis. tHeLa cells overexpressing the FL or the FL with single or multiple mutations were treated with or without 1 μM staurosporine (Sta) during the last 12 h of the 44 h-transfection experiments. The floating and attached cells were harvested together for immunoblotting (5×10^5 cells/lane) with anti-Flag mAb. Close and open circles represent respectively the R-form and the intermediate forms of cleavage products derived from the wild- or mutant-types of NuMA after apoptotic induction. (C) Three apoptotic cutting sites of NuMA at the residues of D^{1705}, D^{1726}, and D^{1747}. TM4 or its single mutants were used for the cleavage assay with a similar experimental design in (B). The numbers of 1, 4, 5 refer to the cleavage products generated at the cutting sites of aspartate residues as those marked in (A). The "x" represents a fragment derived from TM4 or TM4 mutants cleaved at an unidentified apoptotic cutting site. The degraded products from TM4-D4A migrated faster than did the other corresponding fragments, due to different constructions at the multiple cloning sites resulting in loss of a 22-amino-acid-sequence only in TM4-D4A. (D) Inhibitor experiments. As in (C), TM4-D1A and TM4-D4A were used to test their resistance to the staurosporine-induced cleavage in the presence of caspase-3 inhibitor z-DEVD-fmk (100 μM) or caspase-6 inhibitor z-VEID-fmk (100 μM). The labeling letter and numbers for the degraded fragments are the same as in (C).

Figure 1A) to test whether this mutant could resist the cleavage after apoptotic induction. As expected, TM1 remained intact in transiently transfected tHeLa cells treated with staurosporine, DRB, or adriamycin (Figure 3A). Furthermore, immunofluorescence staining showed that cells expressing TM1 maintained the normal nuclear morphology after treatment with staurosporine (Figure 3B, see arrows). We carefully evaluated percentages of apoptosis as determined by DNA condensation and micronucleation in transfected and untransfected cells upon apoptotic induction in five independent experiments. Results clearly demonstrated that the TM1, but not the FL, almost completely prevented cells from the staurosporine-induced nuclear disruption; near 100% protection by TM1 was also observed in DRB- and adriamycin-treated cells (Figure 3C). It should be addressed that all the nine NuMA mutants that did not resist to the apoptotic cleavage (see Figure 2B) showed no protection of the nuclear structure (data not shown).

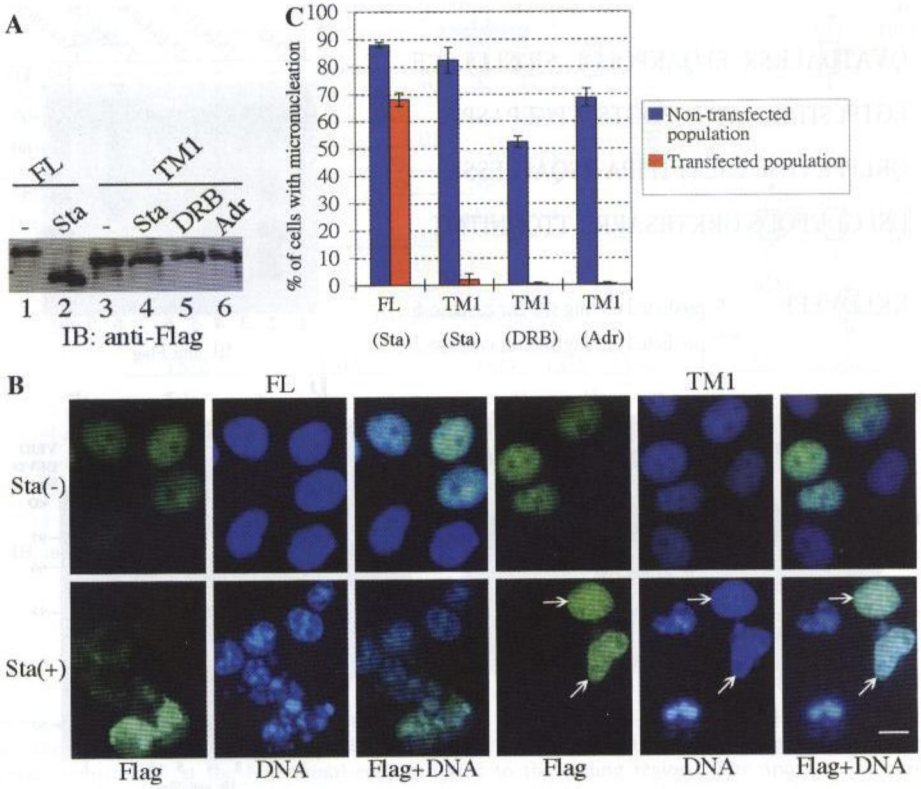

Figure 3. A mutant of NuMA missing amino acids 1701–1828 resists to the apoptotic cleavage and maintains the nuclear integrity. (A) Immunoblot analysis. tHeLa cells were transfected with FL or TM1 and incubated for 44 h; 1 μM staurosporine (Sta), 0.25 mM DRB, or 4 μg/ml adriamycin (Adr) were added to the cultures during the last 12 h. The cell lysates (floating and adherent populations) were analyzed by immunoblotting (5×10^5 cells/lane) using anti-Flag mAb. (B) Immunofluorescence. With the same experimental design in (A), the attached cells after staurosporine treatment were subjected to immunofluorescence staining with anti-Flag. DNA was co-stained with Hoechst 33258. Untreated cells served as the control. Arrows mark the TM1-expressing cells that resisted to the staurosporine treatment. (C) Effects of FL or TM1 on preventing micronucleation. Using the similar experimental design in (A) and (B), ~300 cells of transfected and untransfected populations were evaluated for micronucleation upon treatments with staurosporine, DRB, or adriamycin. Note that near 100% of TM1-expressing cells show no micronucleation upon apoptotic attack. Values are the mean (±SD) of five experiments. Bar, 10 μm.

The NuMA mutant missing the amino acids 1701–1828 does not prevent cytochrome c release but attenuates the late events during apoptosis

We then analyzed apoptotic events of cells expressing the non-cleavable mutant of NuMA, TM1. Staurosporine treatment induced cytochrome *c* release from mitochondria to the cytosol and nucleus (Figure 4A; for the normally punctate distribution of cytochrome *c* in cytoplasm, see untransfected cells in Figure 5E). Neither the FL nor the TM1 prevented cytochrome *c* release, but only the TM1 protected cells from micronucleation (Figure 4A, arrows). One antibody specific to the cleaved active caspase-3 was applied to stain cells using a similar experimental design. Untransfected cells and the FL-expressing cells were strongly positive, while cells expressing TM1 were weakly positive, in the staurosporine-induced caspase-3 activation (Figure 4B, arrows for TM1 expressing cells). We then examined the 85 kD cleavage product of PARP, which is a well-known substrate for caspase-3 [29]. Consistent with the degrees of caspase-3 activation, staurosporine-induced PARP degradation exhibited a much less extent in cells expressing TM1 as compared with those expressing FL or those untransfected (Figure 4C). In TUNEL assays for detecting DNA fragmentation induced by staurosporine, cells untransfected or expressing FL showed much stronger incorporation of biotin-labeled dUTP than did the TM1-transfected cells (Figure 4D).

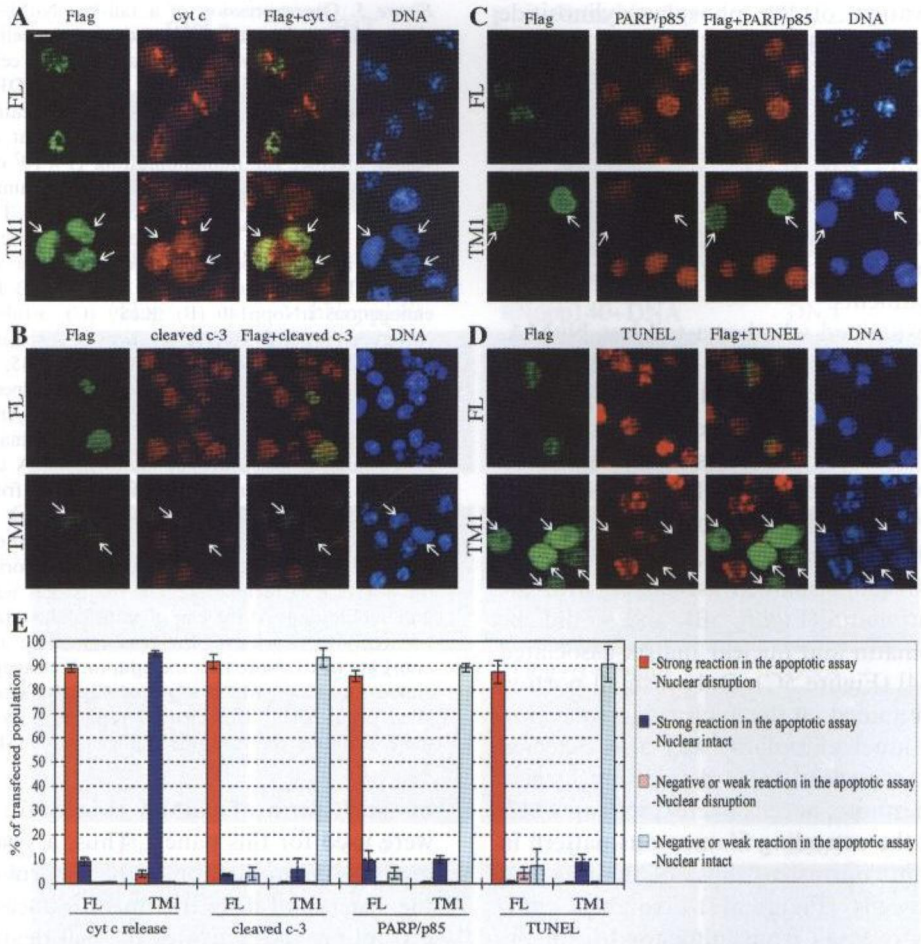

Figure 4. A mutant of NuMA missing amino acids 1701–1828 does not block cytochrome *c* release, but attenuates the late apoptotic events. A similar experimental design to that shown in the Figure 3B was applied to score cells that remained attached to the coverslips after staurosporine treatment. The ectopic expression of FL or TM1 was monitored by anti-Flag (A–D), whereas the endogenous cytochrome *c* (cyt *c*; A), active form of caspase-3 (cleaved c-3; B), the 85 kD fragment of PARP (PARP/p85; C), DNA fragmentation (TUNEL; D) were detected by specific antibodies. DNA was co-stained with Hoechst 33258. Arrows mark cells expressing TM1. (E) Comparison of the FL- and TM1-transfected populations. As shown in (A–D), ~200 transfected cells from each of the eight groups were scored as either strong or weak (including negative) reactions in the four types of apoptotic assays and further classified into subgroups either nuclear disruption or nuclear intact. Values are the mean (±SD) of three experiments. Bar, 10 μm.

Again, TM1 protected cells from nuclear disruption (Figure 4D, arrows). Figure 4E shows statistic scores of three experiments that evaluate only the successfully transfected cells. Effects of the FL versus the TM1 on the staurosporine-induced apoptosis were determined by the four types of apoptotic assays as well as frequencies of micronucleation. The non-cleavable mutant TM1, unable to prevent the drug-induced cytochrome *c* release, could attenuate the subsequent death signaling events, such as activation of caspase-3 (cleaved c-3), generation of the 85 kD product of PARP (PARP/p85), and DNA fragmentation (TUNEL) (light blue bars). Because only the TM1-expressing cells showed nearly complete protection on nuclei after apoptotic induction (combined dark and light blue bars in each groups), it is possible that maintenance of the nuclear integrity by TM1 may eliminate the DNA-damage-based apoptotic signal amplification.

The tail-less NuMA induces chromatin condensation and activates cell death machinery

Previous studies have shown that SV40 large T antigen inhibits apoptosis [30, 31], likely mediated

through activation of the phosphatidylinositide 3′-OH kinase/Akt pathway [32]. The 293T cells, carrying the SV40 large T antigen, represent a model system that can activate the cell survival machinery under stress. Unlike the tHeLa, 293T cells showed that the cleavage of NuMA was not obvious (Figure 5A; Ku80 was not cleaved during apoptosis and served as a loading control) and that the nuclear architecture remained normal (data not shown) after drug treatments.

We then examined whether a tail-less NuMA, TM7 (encoding amino acids 1–1738, mimicking the R-form), by itself could induce disruption of the nucleus in the 293T cell model system of which the cellular survival pathways were activated under stress. Overexpression of TM7 in 293T cells induced chromatin condensation (Figure 5B–H, arrows). Under such conditions, a nucleolar protein hNopp140 [26] remained associated with the condensed chromatin (Figure 5B), and so did the Ku80, a chromatin and nuclear matrix-associated protein [33, 34] (Figure 5C). Only a small portion of Ku80 was retained on the nuclear matrix region where the residual chromatin was also detected (Figure 5C, the nuclear areas defined by broken circles). Furthermore, in cells overexpressing TM7, α-tubulin lost the extending filamentous pattern in cytoplasm as in contrast to those of the attached untransfected cells (Figure 5D). Notably, cytochrome *c* was released from mitochondria of the TM7 transfected cell, as judged by loss of the punctate staining pattern (Figure 5E). " Rounded up" morphology and cytochrome *c* release are hallmarks of apoptotic cells. We then examined other apoptotic parameters for cells overexpressing TM7, such as the cleaved active caspase-3 (Figure 5F), the 85 kD cleavage product of PARP (Figure 5G), and DNA damage by TUNEL assay (Figure 5H). All parameters indicated that TM7 by itself induced apoptosis in 293T cells, a cell line clearly insensitive to many apoptotic inducers. Note that the neighboring untransfected cells were negative for all the apoptotic reactions. It should be addressed that, instead of micronucleation, large DNA clumps due to chromatin condensation were constantly observed in cells expressing TM7. We also found that both the condensed and the residual chromatin regions of the TM7-transfected cells were TUNEL positive (Figure 5H, the disrupted nuclei marked by broken circles). Importantly, the protein size of TM7 was similar to that of the R-form of NuMA (Figure 5I; tHeLa cells were used for this panel). Thus, a system mimicking the overproduction of the R-form of NuMA in the absence of drug treatment induces the nuclear disruption and activates the cell death machinery that apparently bypasses the protective effects mediated by SV40 large T antigen.

Figure 5. Overexpression of a tail-less NuMA TM7 induces▶ chromatin condensation and activates the cell death machinery. (A) Immunoblotting. tHeLa and 293T cells were treated with 1 μM staurosporine (Sta), 0.25 mM DRB, or 4 μg/ml adriamycin (Adr) for 12 h. Cells without treatment (–) served as the control. The detached and adherent cells were harvested together for immunoblotting (1×10^5 cells/lane) using anti-NuMA and anti-Ku80 mAb. (B–H) Immunofluorescence analysis. 293T cells were transfected with TM7 (a tail-less NuMA). After 44 h, cells on the coverslips were examined by double immunofluorescence staining. The ectopically expressed TM7 was monitored by anti-Flag (B–H), whereas the endogenous hNopp140 (B), Ku80 (C), α-tubulin (D), cytochrome *c* (cyt *c*; E), the active form of caspase-3 (cleaved c-3; F), the 85 kD fragment of PARP (PARP/p85; G), DNA fragmentation (TUNEL; H) were detected by specific antibodies. DNA was co-stained with Hoechst 33258. Arrows point out the TM7-expressing cells; broken circles mark the nuclear areas, each of which defines the large DNA clumps together with the residual chromatin region derived from a single nucleus. (I) Comparison between the tail-less TM7 and the R-form of NuMA. tHeLa cells with or without transfection with TM7 were treated with 1 μM staurosporine (Sta) during the last 12 h of incubation. The cell lysates were analyzed by immunoblotting. At the end of transfer the nitrocellulose filter was cut into two halves for detection using anti-NuMA and anti-Flag mAb. Note that the apoptotic cleavage of TM7 generated a product, which migrated slightly faster than the original uncut TM7. This cleaved product is likely identical to the R-form derived from the endogenous NuMA. Bar, 10 μm.

Discussion

Our current study demonstrates that four apoptotic cutting sites are clustered in a nearby region at a junction between the C-terminal globular tail- and the central coiled coil-domains of NuMA, and that NuMA cleavage at its C-terminus is involved in amplification of the downstream apoptotic events. It suggests that one of the nuclear functions of NuMA is for regulating the process of apoptosis.

The cleavage of NuMA leads to disruption of the nuclear architecture

Links between NuMA cleavage and nuclear morphological changes during apoptosis are unclear. Immunoelectron microscopy indicates that NuMA

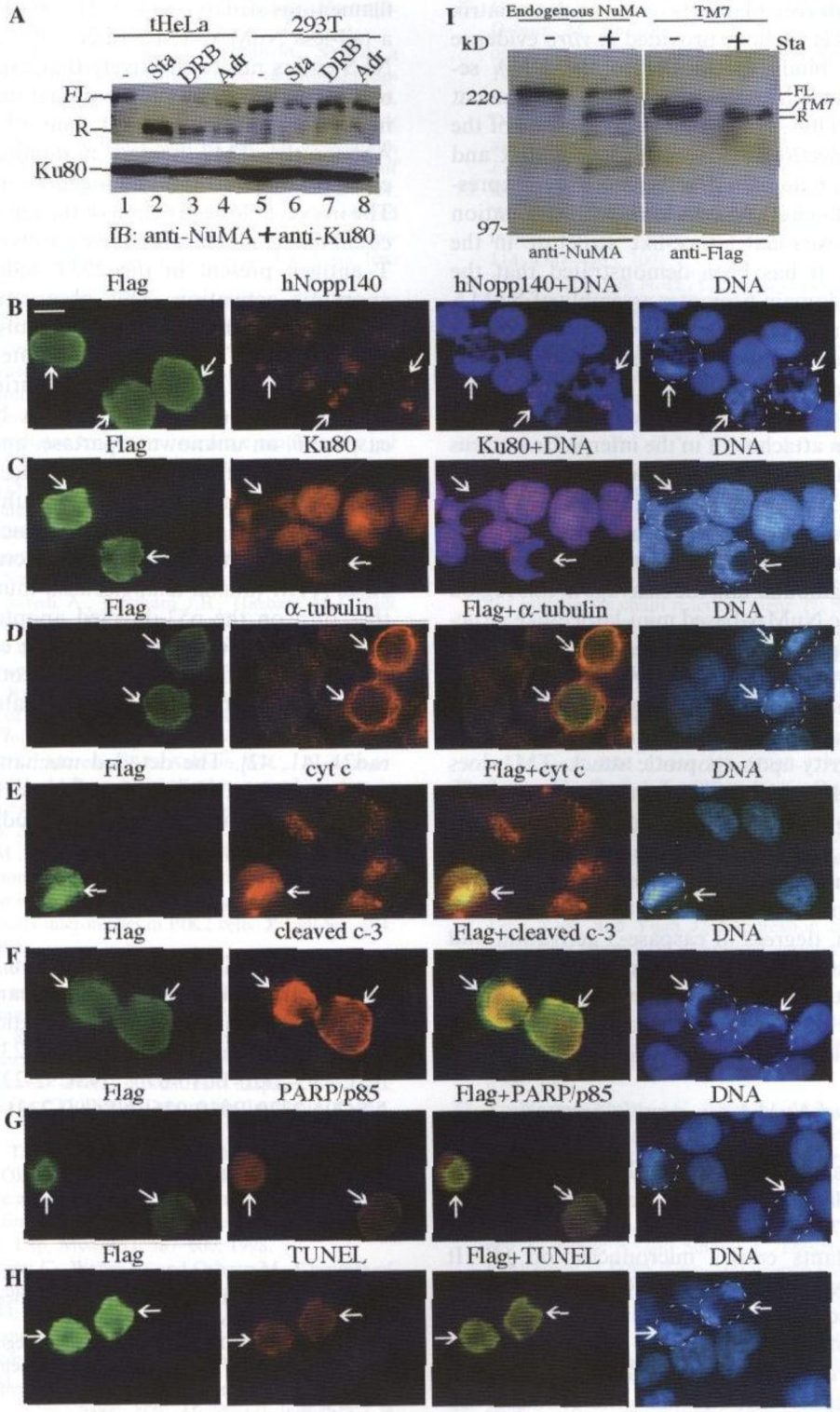
A
tHeLa
293T
- Sta DRB Adr - Sta DRB Adr
FL
R
Ku80
1 2 3 4 5 6 7 8
IB: anti-NuMA + anti-Ku80
I
Endogenous NuMA
TM7
kD - + - + Sta
220
97
FL
TM7
R
anti-NuMA
anti-Flag
Flag
hNopp140
hNopp140+DNA
DNA
B
Flag
Ku80
Ku80+DNA
DNA
C
Flag
α-tubulin
Flag+α-tubulin
DNA
D
Flag
cyt c
Flag+cyt c
DNA
E
Flag
cleaved c-3
Flag+cleaved c-3
DNA
F
Flag
PARP/p85
Flag+PARP/p85
DNA
G
Flag
TUNEL
Flag+TUNEL
DNA
H

associates with core filaments of the nuclear matrix [35]. Ludérus et al. have provided *in vitro* evidence that NuMA binds specifically to the DNA sequences, termed matrix or scaffold attachment regions [36]. Thus, NuMA may serve as one of the physical connections between nuclear matrix and chromatin loop domain. Furthermore, overexpression of the full-length NuMA leads to the formation of a quasi-hexagonal lattice-like structure in the nucleus [21]. It has been demonstrated that the globular tail domain promotes assembly of NuMA into multiarm oligomers [22], and that NuMA mutants with incomplete globular tail domain can cause chromatin mislocalization [21]. These observations imply that NuMA may play a structural role for chromatin attachment in the interphase nucleus and its globular tail domain should be involved in this function. Because the apoptotic cleavage sites have been mapped to the amino acids 1701–1828 of NuMA, at the junction between the α-helical coiled coils and the globular tail, the cleavage in this region may cause the NuMA-based mini-lattice-like structures to collapse. The irreversible destruction of the nuclear matrix could induce DNA fragmentation and micronucleation. Conversely, the uncleavable NuMA mutant such as TM1 can maintain the nuclear integrity upon apoptotic attack. TM1 does not prevent the initial event of cytochrome *c* release after apoptotic attack; it maintains the nuclear integrity and, thereby, blocks the subsequent signal amplification derived from the DNA damage-induced apoptosis. Consistent with this attenuation phenomenon, degrees of caspase-3 activation and PARP cleavage have been found to decrease to a much less extent in the TM1 expressing cells. These observations further support that NuMA plays a structural role in interphase nucleus.

The R-form of NuMA can amplify apoptosis

The appearance of truncated NuMA correlates with DNA laddering and nuclear fragmentation [15, 18, 19, 37] and overexpression of tail-truncated NuMA mutants causes micronucleation [4]. It raises a question whether the R-form of NuMA by itself could induce the irreversible destruction of the nuclear structure that might lead to activation of the cell death machinery. It is known that NuMA mutants without the endogenous NLS (amino acid 1987–2005 in the tail domain) remain in the cytoplasm to form large aggregates or filamentous structures [4, 9, 21, 38]. We found that a tail-less NuMA, TM7, fused with an exogenous NLS enters nuclei effectively that can cause chromatin condensation and apoptotic induction even in the apoptotic resistant line of 293T cells. Apparently, TM7 possess a dominant negative effect to compete off the endogenous intact NuMA. The irreversible destruction of the nuclear structure could overcome the protective effects of SV40 large T antigen present in the 293T cells and led to apoptotic activation. This observation supports that the R-form of NuMA, a tail-less product similar to the TM7, may accelerate the nuclear collapse once it has accumulated during apoptosis. The apoptotic cleavage of NuMA by caspase-3, caspase-6, an unknown aspartase, and an unidentified non-caspase proteinase produces the tail-less NuMA that could amplify the death signal(s) via the DNA damage-induced caspase activation. It is known that damaged chromatin recruits and activates ATM (ataxia-telangiectasia-mutated) to further turn on the p53-directed apoptotic pathway [39, 40]. Therefore, death signaling can be amplified. The amplification of the apoptotic signals has also been observed in other truncated substrates catalyzed by caspases, including vimentin and rad21 [41, 42]. The detailed mechanism how the tail-less NuMA (R-form) activates the cell death machinery remains to be further studied.

Acknowledgements

We thank Y.-T Tsai and C.-I. Lin for critically reading the manuscript. This research was supported by grants from the National Science Council, Taiwan, ROC (NSC94-2320-B010-057; NSC 93-2320-B010-070; NSC92-2320-B010-057; NSC91-2320-B010-036; NSC90-2321-B010-003).

References

1. Cleveland D.W., NuMA: a protein involved in nuclear structure, spindle assembly, and nuclear re-formation. Trends Cell Biol. 5: 60–64, 1995.
2. Moreno Díaz De La Espina S., Samaniego R., Yu W. and De La Torre C., Intermediate filament proteins with nuclear functions: NuMA, lamin-like proteins and MFP1. Cell Biol. Int. 27: 233–235, 2003.
3. Toivola D.M., Tao G.-Z., Habtezion A., Liao J. and Omary M.B., Cellular integrity plus: organelle-related and

protein-targeting functions of intermediate filaments. Trends Cell Biol. 15: 608–617, 2005.
4. Gueth-Hallonet C., Weber K. and Osborn M., NuMA: a bipartite nuclear location signal and other functional properties of the tail domain. Exp. Cell Res. 225: 207–218, 1996.
5. Tang T.K., Tang C.C., Chao Y.-J. and Wu C.-W., Nuclear mitotic apparatus protein (NuMA): spindle association, nuclear targeting and differential subcellular localization of various NuMA isoforms. J. Cell Sci. 107: 1389–1402, 1994.
6. Compton D.A. and Luo C., Mutation of the predicted $p34^{cdc2}$ phosphorylation sites in NuMA impair the assembly of the mitotic spindle and block mitosis. J. Cell Sci. 108: 621–633, 1995.
7. Compton D.A. and Cleveland D.W., NuMA is required for the proper completion of mitosis. J. Cell Biol. 120: 947–957, 1993.
8. Du Q., Stukenberg P.T. and Macara I.G., A mammalian partner of inscuteable binds NuMA and regulates mitotic spindle organization. Nat. Cell Biol. 3: 1069–1075, 2001.
9. Haren L. and Merdes A., Direct binding of NuMA to tubulin is mediated by a novel sequence motif in the tail domain that bundles and stabilizes microtubules. J. Cell Sci. 115: 1815–1824, 2002.
10. Mattagajasingh S.N., Huang S.-C., Hartenstein J.S., Snyder M., Marchesi V.T. and Benz E.J. Jr., A nonerythroid isoform of protein 4.1R interacts with the nuclear mitotic apparatus (NuMA) protein. J. Cell Biol. 145: 29–43, 1999.
11. Gaglio T., Saredi A., Bingham J.B., Hasbani M.J., Gill S.R., Schroer T.A. and Compton D.A., Opposing motor activities are required for the organization of the mammalian mitotic spindle pole. J. Cell Biol. 135: 399–414, 1996.
12. Merdes A., Ramyar K., Vechio J.D. and Cleveland D.W., A complex of NuMA and cytoplasmic dynein is essential for mitotic spindle assembly. Cell 87: 447–458, 1996.
13. Nachury M.V., Maresca T.J., Salmon W.C., Waterman-Storer C.M., Heald R. and Weis K., Importin β is a mitotic target of the small GTPase Ran in spindle assembly. Cell 104: 95–106, 2001.
14. Kallajoki M., Harborth J., Weber K. and Osborn M., Microinjection of a monoclonal antibody against SPN antigen, now identified by peptide sequences as the NuMA protein, induces micronuclei in PtK2 cells. J. Cell Sci. 104: 139–150, 1993.
15. Hsu H.-L. and Yeh N.-H., Dynamic changes of NuMA during the cell cycle and possible appearance of a truncated form of NuMA during apoptosis. J. Cell Sci. 109: 277–288, 1996.
16. Andrade F., Roy S., Nicholson D., Thornberry N., Rosen A. and Casciola-Rosen L., Granzyme B directly and efficiently cleaves several downstream caspase substrates: implications for CTL-induced apoptosis. Immunity 8: 451–460, 1998.
17. Hirata H., Takahashi A., Kobayashi S., Yonehara S., Sawai H., Okazaki T., Yamamoto K. and Sasada M., Caspases are activated in a branched protease cascade and control distinct downstream processes in Fas-induced apoptosis. J. Exp. Med. 187: 587–600, 1998.
18. Gueth-Hallonet C., Weber K. and Osborn M., Cleavage of the nuclear matrix protein NuMA during apoptosis. Exp. Cell Res. 233: 21–24, 1997.
19. Taimen P. and Kallajoki M., NuMA and nuclear lamins behave differently in Fas-mediated apoptosis. J. Cell Sci. 116: 571–583, 2003.
20. Kivinen K., Kallajoki M. and Taimen P., Caspase-3 is required in the apoptotic disintegration of the nuclear matrix. Exp. Cell Res. 311: 62–73, 2005.
21. Gueth-Hallonet C., Wang J., Harborth J., Weber K. and Osborn M., Induction of a regular nuclear lattice by overexpression of NuMA. Exp. Cell Res. 243: 434–452, 1998.
22. Harborth J., Wang J., Gueth-Hallonet C., Weber K. and Osborn M., Self assembly of NuMA: multiarm oligomers as structural units of a nuclear lattice. EMBO J. 18: 1689–1700, 1999.
23. Harborth J., Elbashir S.M., Bechert K., Tuschl T. and Weber K., Identification of essential genes in cultured mammalian cells using small interfering RNAs. J. Cell Sci. 114: 4557–4565, 2001.
24. Li L.-L. and Yeh N.-H., Cell cycle-dependent migration of the DNA-binding protein Ku80 into nucleoli. Exp. Cell Res. 199: 262–268, 1992.
25. Pai C.-Y., Chen H.-K., Sheu H.-L. and Yeh N.-H., Cell-cycle-dependent alterations of a highly phosphorylated nucleolar protein p130 are associated with nucleologenesis. J. Cell Sci. 108: 1911–1920, 1995.
26. Chen H.-K., Pai C.-Y., Huang J.-Y. and Yeh N.-H., Human Nopp140, which interacts with RNA polymerase I: implications for rRNA gene transcription and nucleolar structural organization. Mol. Cell. Biol. 19: 8536–8546, 1999.
27. Ho S.N., Hunt H.D., Horton R.M., Pullen J.K. and Pease L.R., Site-directed mutagenesis by overlap extension using the polymerase chain reaction. Gene 77: 51–59, 1989.
28. Thornberry N.A., Rano T.A., Peterson E.P., Rasper D.M., Timkey T., Garcia-Calvo M., Houtzager V.M., Nordstrom P.A., Roy S., Vaillancourt J.P., Chapman K.T. and Nicholson D.W., A combinatorial approach defines specificities of members of the caspase family and granzyme B. Functional relationships established for key mediators of apoptosis. J. Biol. Chem. 272: 17907–17911, 1997.
29. Tewari M., Quan L.T., O'Rourke K., Desnoyers S., Zeng Z., Beidler D.R., Poirier G.G., Salvesen G.S. and Dixit V.M., Yama/CPP32β, a mammalian homolog of CED-3, is a CrmA-inhibitable protease that cleaves the death substrate poly(ADP-ribose) polymerase. Cell 81: 801–809, 1995.
30. Jung Y.-K. and Yuan J., Suppression of Interleukin-1β converting enzyme (ICE)-induced apoptosis by SV40 large T antigen. Oncogene 14: 1207–1214, 1997.
31. Slinskey A., Barnes D. and Pipas J.M., Simian virus 40 large T antigen J domain and Rb-binding motif are sufficient to block apoptosis induced by growth factor withdrawal in a neural stem cell line. J. Virol. 73: 6791–6799, 1999.
32. Yu Y. and Alwine J.C., Human cytomegalovirus major immediate-early proteins and simian virus 40 large T antigen can inhibit apoptosis through activation of the phosphatidylinositide 3'-OH kinase pathway and the cellular kinase Akt. J. Virol. 76: 3731–3738, 2002.
33. Koike M., Awaji T., Kataoka M., Tsujimoto G., Kartasova T., Koike A. and Shiomi T., Differential subcellular localization of DNA-dependent protein kinase components Ku and DNA-PKcs during mitosis. J. Cell Sci. 112: 4031–4039, 1999.
34. Yu E., Song K., Moon H., Maul G.G. and Lee I., Characteristic immunolocalization of Ku protein as nuclear matrix. Hybridoma 17: 413–420, 1998.
35. Zeng C., He D. and Brinkley B.R., Localization of NuMA protein isoforms in the nuclear matrix of mammalian cells. Cell Motil. Cytoskel. 29: 167–176, 1994.

36. Ludérus M.E.E., den Blaauwen J.L., de Smit O.J.B., Compton D.A. and van Driel R., Binding of matrix attachment regions to lamin polymers involves single-stranded regions and the minor groove. Mol. Cell. Biol. 14: 6297–6305, 1994.
37. Weaver V.M., Carson C.E., Walker P.R., Chaly N., Lach B., Raymond Y., Brown D.L. and Sikorska M., Degradation of nuclear matrix and DNA cleavage in apoptotic thymocytes. J. Cell Sci. 109: 45–56, 1996.
38. Saredi A., Howard L. and Compton D.A., NuMA assembles into an extensive filamentous structure when expressed in the cell cytoplasm. J. Cell Sci. 109: 619–630, 1996.
39. Kurz E.U. and Lees-Miller S.P., DNA damage-induced activation of ATM and ATM-dependent signaling pathways. DNA Repair 3: 889–900, 2004.
40. Miller F.D., Pozniak C.D. and Walsh G.S., Neuronal life and death: an essential role for the p53 family. Cell Death Differ. 7: 880–888, 2000.
41. Byun Y., Chen F., Chang R., Trivedi M., Green K.J. and Cryns V.L., Caspase cleavage of vimentin disrupts intermediate filaments and promotes apoptosis. Cell Death Differ. 8: 443–450, 2001.
42. Pati D., Zhang N. and Plon S.E., Linking sister chromatid cohesion and apoptosis: Role of Rad21. Mol. Cell. Biol. 22: 8267–8277, 2002.